

Near Zone Navier-Stokes Analysis of Heavy Quark Jet Quenching in an $\mathcal{N} = 4$ SYM Plasma

Jorge Noronha^{1,2,3}, Giorgio Torrieri², and Miklos Gyulassy¹

¹*Department of Physics, Columbia University, 538 West 120th Street, New York, NY 10027, USA*

²*Institut für Theoretische Physik, J.W. Goethe-Universität,
Max-von-Laue-Str. 1, 60438 Frankfurt am Main, Germany*

³*Frankfurt Institute for Advanced Studies, J.W. Goethe-Universität,
Ruth-Moufang-Str. 1, 60438 Frankfurt am Main, Germany*

(Dated: June 29, 2021)

The near zone energy-momentum tensor of a supersonic heavy quark jet moving through a strongly-coupled $\mathcal{N} = 4$ SYM plasma is analyzed in terms of first-order Navier-Stokes hydrodynamics. It is shown that the hydrodynamical description of the near quark region worsens with increasing quark velocities. For realistic quark velocities, $v = 0.99$, the non-hydrodynamical region is located at a narrow band surrounding the quark with a width of approximately $3/\pi T$ in the direction parallel to the quark's motion and with a length of roughly $10/\pi T$ in the perpendicular direction. Our results can be interpreted as an indication of the presence of coherent Yang-Mills fields where deviation from hydrodynamics is at its maximum. In the region where hydrodynamics does provide a good description of the system's dynamics, the flow velocity is so small that all the nonlinear terms can be dropped. Our results, which are compatible with the thermalization timescales extracted from elliptic flow measurements, suggest that if AdS/CFT provides a good description of the RHIC system, the bulk of the quenched jet energy has more than enough time to locally thermalize and become encoded in the collective flow. The resulting flow pattern close to the quark, however, is shown to be considerably different than the superposition of Mach cones and diffusion wakes observed at large distances.

I. INTRODUCTION

One of the most prominent experimental discoveries made at the Relativistic Heavy Ion Collider (RHIC) has been the suppression of highly energetic particles [1, 2, 3, 4], which suggests that the matter created at RHIC is a color-opaque, high density medium of colored particles where fast partons quickly lose energy by gluon emission [5, 6, 7, 8]. Measurements of anisotropies in soft particle momentum distributions [1, 2, 3, 4] have further indicated that soft degrees of freedom are approximately thermalized. The degree of thermalization has been found to be considerably above the predictions obtained within perturbative quantum chromodynamics (QCD) [9] and, in fact, it seems to be compatible with the “perfect fluid” scenario where the strongly-coupled quark-gluon plasma (sQGP) has almost zero viscosity [10, 11, 12, 13, 14, 15]. This indicates that perturbative methods may fail at describing the microscopic properties of the matter created in ultrarelativistic heavy ion collisions.

An alternative approach for understanding jet suppression in the sQGP relies on analyzing the similar problem of a heavy quark moving through an $\mathcal{N} = 4$ super Yang-Mills (SYM) plasma. There the Anti-de Sitter/Conformal Field Theory (AdS/CFT) correspondence [16] provides a way to compute observables at strong coupling on the CFT side, such as the stress tensor of the $\mathcal{N} = 4$ SYM plasma, starting from gravitational calculations in five-dimensional AdS space.

It is important to remark that one has to be careful when comparing QCD and $\mathcal{N} = 4$ SYM given that both

the symmetries and the microscopic degrees of freedom are very different. The hope is that some of the differences become unimportant in the strongly coupled limit where the system is to a good approximation a locally thermalized liquid.

A notable result obtained using the AdS/CFT correspondence [17] was that the ratio between the viscosity η and entropy density s of an $\mathcal{N} = 4$ SYM plasma in the limit of large number of colors N_c and large 't Hooft coupling λ converges to a “universal limit”

$$\frac{\eta}{s} = \frac{1}{4\pi}, \quad (1)$$

which has been conjectured [18] to be the lowest value for this ratio obtainable in a physical system. Remarkably, hydrodynamic models find that the viscosity of the system created at RHIC is compatible, or even lower, than this limit [11, 12, 15].

The apparent local thermalization at RHIC suggests the possibility that the energy lost in jets will itself become locally thermalized, i.e., encoded in the local hydrodynamic flow. In the immediate vicinity of the jet the variation of the thermodynamic quantities is probably very large, which means that a hydrodynamic description of the system is bound to fail in this region. The typical length scale associated with this region is, for instance, given by the sound attenuation length $\Gamma = 4\eta/3\omega < 1/\pi T$, where ω is the enthalpy of the medium (see [19]). For distances scales larger than Γ , one expects that the system can be described in terms of nonlinear viscous hydrodynamics. Sufficiently far from the jet, however, the flow velocity and the gradients of the thermodynamic quantities are so small that linearized

hydrodynamic equations should provide an accurate description of the system's dynamics. In the linearized limit, for certain energy deposition patterns, this gives rise to Mach cones, which can be readily connected to the fluid's equation of state [20]. In the absence of these conditions, the flow pattern is likely to be considerably more complex but will nevertheless result in a correlation between the flow and the jet. The possibility of detecting these effects in heavy ion collisions has recently been subject to intense theoretical and experimental interest [21, 22, 23, 24, 25, 26, 27].

The degree of thermalization of the energy of the suppressed jets is a fundamental probe of the microscopic properties of the matter created at RHIC. Because of the apparent strong coupling of the system, non-perturbative methods such as AdS/CFT seem to be necessary. Recently, this method has been used to obtain the energy-momentum tensor of an infinitely heavy quark moving at constant velocity through a strongly coupled plasma [28, 29]. The results have been analyzed in the far field limit [29, 30, 31, 32, 33, 34] in terms of linearized Navier-Stokes hydrodynamics and, encouragingly, it has been shown that structures resembling Mach cones and diffusion wakes, with an angle comparable to that expected from the equation of state, do form in the far-field limit. In fact, in [34] it was shown that linearized Navier-Stokes hydrodynamics provides a very accurate description of the system at distances $\geq 5/\pi T$ (in the limit of the large N_c and λ).

As mentioned above, close to the quark linearized hydrodynamics, and eventually the hydrodynamic description, should fail to account for the energy-momentum tensor of the system. Distinguishing between non-linear, turbulent hydrodynamics, and the failure of hydrodynamics is impossible within the linearized regime. In this work we focus on the region very close to the quark and perform an analysis of the *near quark* energy-momentum tensor computed in [35] (see also [36] and [37]) using viscous, non-linear (first-order) Navier-Stokes hydrodynamics. We construct the flow vector by boosting the energy-momentum tensor in [35] to the local rest frame of the flow. This flow vector is used to construct the energy-momentum tensor corresponding to a viscous fluid having an equation of state and transport coefficients identical to those of strongly coupled $\mathcal{N} = 4$ SYM matter with the same flow vector. We then quantitatively examine the discrepancies between the two tensors and plot them as a function of the distance from the heavy quark.

Throughout this paper the units are $\hbar = c = k_B = 1$ and 4-vectors are denoted by capital letters, e.g., $U^\mu = (U^0, \vec{U})$. Also, the Minkowski metric $g_{\mu\nu} = \text{diag}(-, +, +, +)$ is used.

II. THE NEAR-QUARK ENERGY-MOMENTUM TENSOR

The energy-momentum tensor of a heavy quark passing through an $\mathcal{N} = 4$ SYM plasma at finite temperature T can be computed by considering metric fluctuations due to a string that is hanging down from the boundary of an AdS Schwarzschild (AdS-SS) background geometry [29]¹. In fact, in this limit the total action that describes the supergravity approximation to type IIB string theory in an AdS-SS background and the classical string is given by the sum of the following partial actions

$$A_G = \frac{1}{16\pi G_5} \int \sqrt{-G} \left(R + \frac{12}{L^2} \right) \quad (2)$$

and

$$A_{NG} = -\frac{1}{2\pi\alpha'} \int \sqrt{-G_{\mu\nu}^{(0)} \partial_\alpha X^\mu \partial_\beta X^\nu} d^2\sigma, \quad (3)$$

where L is the radius of AdS_5 , $G_5 = \pi L^2/2N_c^2$, $\alpha' = L^2/\sqrt{\lambda}$, $G_{\mu\nu}$ is the total metric, and $G_{\mu\nu}^{(0)}$ is the metric of the unperturbed AdS-SS black hole (without effects from the string), which can be obtained from

$$ds^2 = \frac{L^2}{z^2} \left(-g(z)dt^2 + d\vec{x}^2 + \frac{dz^2}{g(z)} \right) \quad (4)$$

where z goes from 0 at the AdS boundary to $z_0 = 1/\pi T$ at the black hole horizon (T is the Hawking temperature associated with the black hole) and $g(z) = 1 - (z/z_0)^4$. The string coordinates $X^\mu(\sigma, \tau)$ in the Nambu-Goto action in Eq. (3) are chosen in such a way that the string endpoint (which corresponds to the heavy quark in the 4-dimensional boundary) moves at constant speed v and no energy flows from the horizon into the string [38, 39].

Minimizing the action S with respect to G leads to the full set of Einstein's equations. It is sufficient for our purposes here to consider instead the linearized Einstein's equations for the metric fluctuations $h_{\mu\nu}$, which are defined via $G_{\mu\nu} = G_{\mu\nu}^{(0)} + h_{\mu\nu}$. It can be shown [29, 35] that the contribution from the moving quark to the total energy-momentum tensor is $T_{quark} = \frac{1}{\pi} \sqrt{\frac{\lambda}{1-v^2}} Q$, where the tensor Q is obtained by expanding h in powers of z near the boundary, i.e., $h \sim Q z^4$. The total energy-momentum tensor in the lab frame that describes the near-quark dynamics of the plasma was computed by Yarom [35] and it reads

$$T_{\mu\nu}^Y = P_0 \text{diag}\{3, 1, 1, r^2\} + \Delta T_{\mu\nu}(x_1, r). \quad (5)$$

¹ Fluctuations of the string can be neglected when $M/T \gg \sqrt{\lambda}$, where M is the quark's mass [23, 38, 40]. In this paper we consider only this classical limit. Assuming that $T = 0.5$ GeV and $\lambda = 3\pi$, one sees that the classical string dynamics is a much better approximation for bottom quarks than for charm quarks.

where the explicit form of $\Delta T_{\mu\nu}$ is

$$\begin{aligned}
\Delta T_{tt} &= \alpha \frac{v(r^2(-5 + 13v^2 - 8v^4) + (-5 + 11v^2)x_1^2) x_1}{72(r^2(1 - v^2) + x_1^2)^{5/2}}, \\
\Delta T_{tx_1} &= -\alpha \frac{v^2(2x_1^2 + (1 - v^2)r^2) x_1}{24(r^2(1 - v^2) + x_1^2)^{5/2}}, \\
\Delta T_{tr} &= -\alpha \frac{(1 - v^2)v^2(11x_1^2 + 8r^2(1 - v^2)) r}{72(r^2(1 - v^2) + x_1^2)^{5/2}}, \\
\Delta T_{x_1x_1} &= \alpha \frac{v(r^2(8 - 13v^2 + 5v^4) + (11 - 5v^2)x_1^2) x_1}{72(r^2(1 - v^2) + x_1^2)^{5/2}}, \\
\Delta T_{x_1r} &= \alpha \frac{v(1 - v^2)(8r^2(1 - v^2) + 11x_1^2) r}{72(r^2(1 - v^2) + x_1^2)^{5/2}}, \\
\Delta T_{rr} &= -\alpha \frac{v(1 - v^2)(5r^2(1 - v^2) + 8x_1^2) x_1}{72(r^2(1 - v^2) + x_1^2)^{5/2}}, \\
\Delta T_{\theta\theta} &= -\alpha \frac{r^2 v(1 - v^2) x_1}{9(r^2(1 - v^2) + x_1^2)^{3/2}}. \tag{6}
\end{aligned}$$

and $\alpha = \gamma_q \sqrt{\lambda} \pi^2 T^4$. In the equations above we used the dimensionless cylindrical coordinates $x_1 = X_1 \pi T$ (where $X_1 = X - vt$ is the comoving coordinate of the quark), $r = X_p \pi T$, and also defined $\gamma_q = 1/\sqrt{1 - v^2}$. Moreover, $P_0 = (N_c^2 - 1) \pi^2 T^4 / 8 + \mathcal{O}(N_c^0)$ is the pressure of the ideal SYM plasma [41]. Note that the disturbances in the medium caused by the string are parametrically of $\mathcal{O}(T^2/X^2)$ in the near-quark region [35], while the vacuum Coulomb stress (not included here) is $\mathcal{O}(1/X^4)$ [29].

It is assumed throughout the derivation of Eq. (5) that the metric disturbances caused by the moving string are small in comparison to the AdS_5 background metric. Therefore, this result is correct as long as this condition is fulfilled. In fact, since $\Delta T_{\mu\nu}$ scales inversely with the total distance from the quark, the region where the condition $\Delta T_{\mu\nu}/P_0 < 1$ (or, equivalently, h small in comparison to $G^{(0)}$) holds can be taken to be arbitrarily small as long as the limit where $N_c \rightarrow \infty$ and λ is large is employed. However, in order to evaluate the relevance of this approach to heavy ion collisions, one may choose $N_c = 3$, $\lambda = 3\pi$ ($\alpha_s = 0.25$), and $\gamma_q = 10$. Using these parameters, one obtains that the magnitude of the energy density disturbances caused by the string along the jet axis, $\Delta T_{tt}/(3P_0)|_{r=0}$, is < 1 when $|X_1| > 1/(\pi T)$ (which is comparable to uncertainty principle bound on the mean free path discussed in [9]).

III. COMPARISON TO HYDRODYNAMICS

We shall now compare the tensor in Eq. 5 to the one that represents a solution to the relativistic Navier-Stokes equations with an arbitrary flow. We underline that the *quantitative* values for the flow and thermodynamic quantities resulting from our analysis should be taken with caution. In fact, one would expect that the validity of a low-energy hydrodynamic description of the near-field region worsens as one becomes closer to the heavy quark. However, this analysis is necessary to ascertain the domain of validity of (general) hydrodynamics, as opposed to non-equilibrium field configurations (up to the ‘‘opposite extreme’’ of fully anisotropic classical solutions to the field equations). As we show in this paper and subsequent work [42], ascertaining this domain of validity of hydrodynamics is crucial for the development of the phenomenological properties of AdS/CFT based models.

In hydrodynamics, the Knudsen number K_N is defined as the ratio between the mean free path l_{MFP} and a characteristic spatial dimension of the system q . Hydrodynamics is applicable when $K_N \equiv l_{MFP}/q \ll 1$. In conformal field theories at finite temperature, the only dimensionful parameter is given by the temperature T and, thus, both l_{MFP} and q should be proportional to $1/T$. However, the mean free path is not a well defined quantity in $\mathcal{N} = 4$ SYM theories at very strong coupling. Nevertheless, one can still define an effective Knudsen number as

$$K_N \equiv \Gamma \left| \frac{\vec{\nabla} \cdot \vec{S}}{S} \right| \tag{7}$$

where $\Gamma = 1/3\pi T$ is the sound attenuation length (to leading order in N_c), $S_i = -T_{0i}^Y$ is the momentum density, and $S = \sqrt{\vec{S}^2}$. Note that this quantity does not depend on N_c and λ but it strongly depends on v . It is illustrated in Fig. 1 how K_N changes with v . For $v = 0.75$, $K_N \ll 1$ practically everywhere but in a small region of radius $\sim 1/\pi T$ that surrounds the quark. However, when v takes more realistic values, say, $v = 0.99$, $K_N \gtrsim 1$ in a narrow region located at $-3/\pi T < X_1 < 3/\pi T$ and $X_p > 0$. Therefore, one can expect that in this region the system cannot be described by hydrodynamics.

Another way to verify whether the system described by the energy-momentum tensor in Eq. (5) admits a hydrodynamic description is to compute its flow vector U^μ , which can be obtained by boosting to the Landau frame where $(T_{0i}^Y)_L = 0$ (denoted henceforward by brackets and subscript L , $(\dots)_L$). Note that, unless the system is a *coherent* field where the phase velocity is equal to the speed of light (such would be the case of an electromagnetic wave), this transformation is always possible. It can be accomplished by solving a system of two equations for the two space-like components of U^μ , U_1 and U_r ($U_\theta = 0$),

$$(T_{0i}^Y)_L = \Lambda_i^\mu T_{\mu\nu}^Y \Lambda_0^\nu = 0, \tag{8}$$

where Λ_i^μ is a general coordinate dependent Lorentz

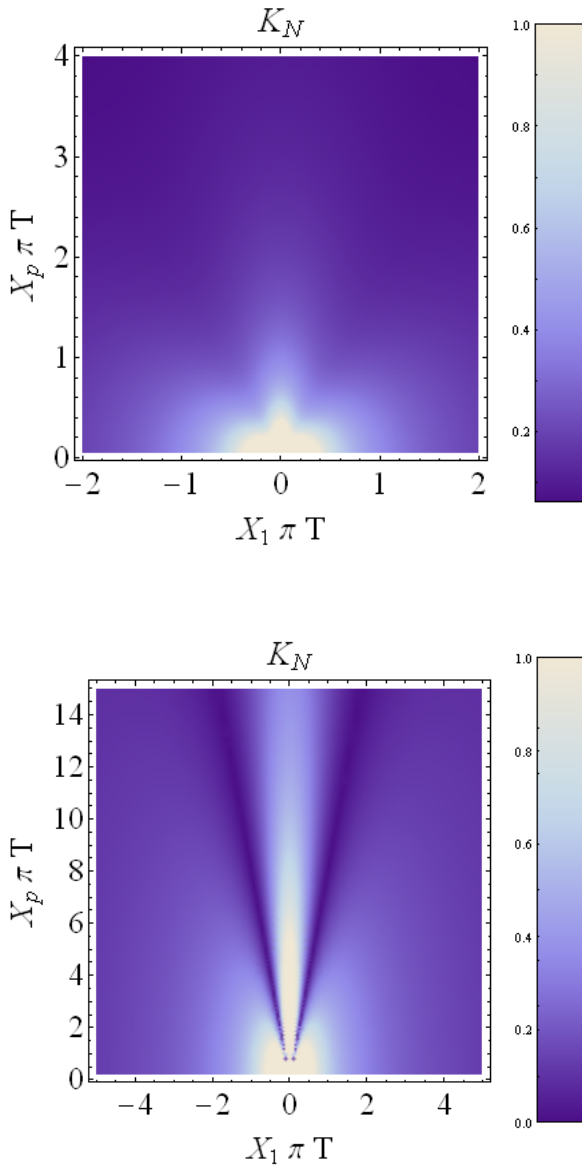


FIG. 1: (Color online) Effective knudsen number for $v = 0.75$ (left panel) and $v = 0.99$ (right panel). Note that different scales were used in the left and right panels. Ratio values outside of the limits were color-coded as the limits.

transformation

$$\Lambda = \begin{pmatrix} \gamma & \vec{U}^T \\ \vec{U} & 1 + \frac{\vec{U} \otimes \vec{U}^T}{\vec{U}^2} (\gamma - 1) \end{pmatrix}, \quad (9)$$

where $\gamma \equiv U^0 = \sqrt{1 + \vec{U}^2}$. Using the representation

$$T^Y = \begin{pmatrix} \varepsilon & -\vec{S}^T \\ -\vec{S} & \hat{\tau} \end{pmatrix} \quad (10)$$

where $\varepsilon = T_{00}^Y$ and $\hat{\tau}_{ij} = T_{ij}^Y$ ($i, j = 1, 2, 3$), we obtain

that Eq. (8) becomes

$$\vec{U} = \frac{1}{(\gamma \varepsilon - \vec{S}^T \cdot \vec{U})} \left[1 + \frac{\vec{U} \otimes \vec{U}^T}{\vec{U}^2} (\gamma - 1) \right] (\gamma \vec{S} - \hat{\tau} \vec{U}). \quad (11)$$

For finite N_c and λ this equation can only be solved numerically. However, for very large N_c and large λ one can use that, to leading order in $1/N_c$, $\gamma \approx 1$, $\varepsilon \approx 3P_0$, and $\hat{\tau} \approx P_0$. Using these approximations, one can then obtain that

$$\vec{U} \approx \frac{\vec{S}}{4P_0}. \quad (12)$$

In deriving the equation above we used that $\sqrt{\lambda}/N_c^2 \ll 1$. The fact that $|\vec{U}| \sim \mathcal{O}(\sqrt{\lambda}/N_c^2)$ in the large N_c , λ limit implies that nonlinear terms in the hydrodynamic description are subleading contributions that can be neglected. Thus, if the system's dynamics can be described by hydrodynamics, these equations have to be linear for the present string theory setup obtained in the large N_c , λ limit [43]. However, at finite N_c and λ nonlinear effects are expected to be relevant. These nonlinear effects can only be properly taken into account by incorporating subleading $1/N_c$ corrections. Because these corrections have yet to be calculated, we shall extrapolate the validity of our leading order results and make a comparison between the near-quark energy-momentum tensor in Eq. (5) and a hydrodynamic ansatz using the phenomenologically relevant set of parameters $N_c = 3$ and $\lambda = 3\pi$. In this work, to estimate both the non-linearities and non-equilibrium effects in the near-zone, we shall use the non-linear ansatz in Eq. (11) rather than Eq. (12).

The energy-momentum tensor of a viscous fluid containing no conserved charges can be parametrized using the energy density ρ , pressure p , and energy flow vector U^μ [20]

$$T_{\mu\nu}^{NS} = (\rho + p) U_\mu U_\nu + p g_{\mu\nu} + \Pi_{\mu\nu} \quad (13)$$

(in our metric convention $U_\mu U^\mu = -1$). $\Pi^{\mu\nu}$ is the shear tensor, which contains the corrections to local thermalization that can be expanded in terms of the gradients of U^μ . To first-order in these gradients (Navier-Stokes limit), this tensor is given by [20]

$$\begin{aligned} \Pi^{\mu\nu} = & -\eta (\partial^\mu U^\nu + \partial^\nu U^\mu + U^\mu U_\alpha \partial^\alpha U^\nu \\ & + U^\nu U^\alpha \partial_\alpha U^\mu) + \frac{2}{3} \eta \Delta^{\mu\nu} (\partial_\alpha U^\alpha), \end{aligned} \quad (14)$$

where $\Delta^{\mu\nu} = g^{\mu\nu} + U^\mu U^\nu$ is the local spatial projector and $\eta = (N_c^2 - 1) \pi T^3 / 8$. Note that we kept the nonlinear terms in U^μ in the definition of $\Pi_{\mu\nu}$.

Once the solution to \vec{U} has been found (by solving the transcendental equation (11) numerically), the shear tensor $\Pi_{\mu\nu}$ and the energy-momentum tensor $T_{\mu\nu}^{NS}$ can be computed from Eqs. (14) and (13). The continuity of $\Pi_{\mu\nu}$ confirms the stability of our numerical solution and the existence of only one physically relevant set of \vec{U} .

For an inviscid fluid, the form of the transformed tensor will be

$$(T_{\mu\nu}^{id})_L = \text{diag}\{\rho, p, p, p\}. \quad (15)$$

If the first-order Navier-Stokes approximation provides a full description of the system,

$$(T_{\mu\nu}^Y)_L = (T_{\mu\nu}^{NS})_L = (T_{\mu\nu}^{id})_L + (\Pi^{\mu\nu})_L \quad (16)$$

where

- $(\Pi^{\mu\nu})_L$ is the shear tensor of Eq. (14) transformed to the Landau frame.
- ρ in Eq. (15) is given by

$$\rho(x_1, r) = (T_{00}^Y)_L - (\Pi_{00})_L \quad (17)$$

- The equation of state is the CFT one, $p = \rho/3$.

Note that Eq. (15) can in general be very different than the “background” tensor $\langle T_{plasma} \rangle = P_0 \text{diag}\{3, 1, 1, r^2\}$, since it is defined in the frame *comoving* with the flow generated by the jet.

The deviation from Navier-Stokes hydrodynamics can then be quantitatively investigated by defining the tensor

$$Z_{\mu\nu} = T_{\mu\nu}^Y - \Pi_{\mu\nu} \quad (18)$$

and studying, in particular, discrepancies between $(Z^{\mu\nu})_L$ and $(T_{\mu\nu}^{id})_L$. If $(T_{\mu\nu}^Y)_L$ corresponds to a solution of the Navier-Stokes equations, we should get

$$(Z_{11})_L = (Z_{22})_L = (Z_{33})_L = \frac{1}{3} (Z_{00})_L, \quad (19)$$

and

$$(Z_{ij})_L = 0. \quad (20)$$

IV. RESULTS

In this preliminary analysis, we will concentrate on the case where $\lambda = 3\pi$, $N_c=3$, and the quark velocity in the lab frame is $v = 0.99$. We would like to remark at this point that $1/\pi T$ is the natural uncertainty principle bound on spatial resolution at temperature T in an ultrarelativistic plasma and provides a lower bound on the mean free path and hence viscosity [9]. Within a radius $1/\pi T$ of the quark jet our semiclassical dissipative fluid analysis is expected to fail and non-equilibrium and field coherence effects may dominate the dynamics.

The plot seen in Fig. 2 immediately illustrates that the flow nearby the quark is very different than a superposition of a Mach cone and a diffusion wake (\vec{V} is such that $\vec{U} = \gamma\vec{V}$). Note that $\vec{V}^2 < 1$ everywhere. This structure is expected to be somewhat stable with respect to v since viscosity results in a length scale below which the fluid “sticks” to and co-moves with the quark. In

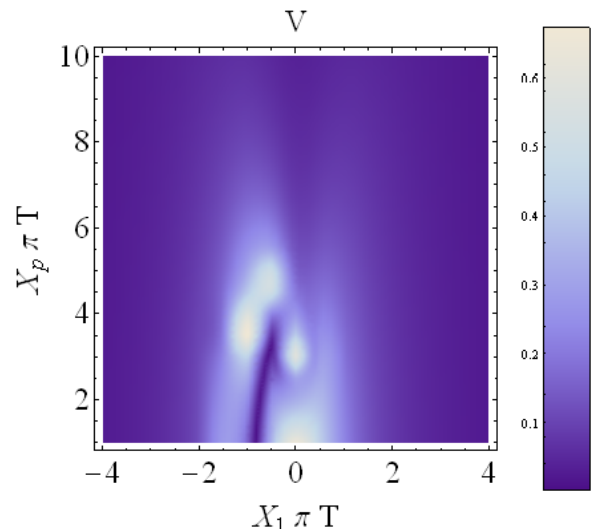


FIG. 2: (Color online) Contour plot of the magnitude of the non-relativistic flow velocity \vec{V} for $v = 0.99$.

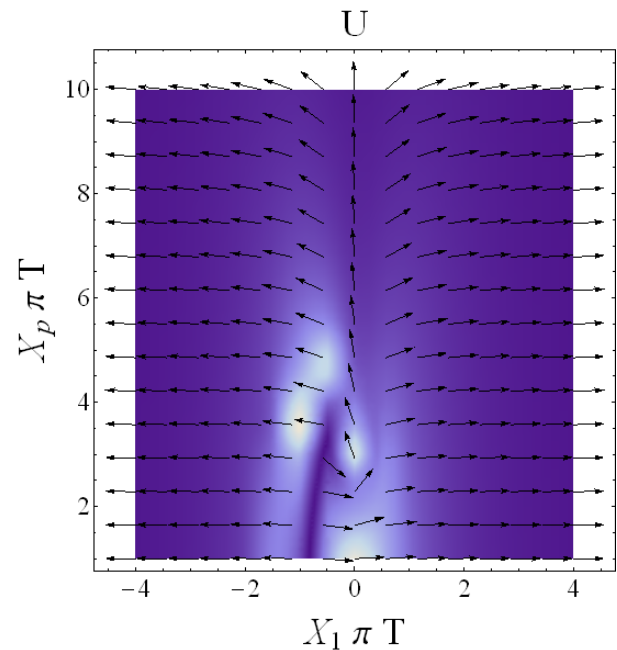


FIG. 3: (Color online) Contour plot of the collective flow \vec{U} for $v = 0.99$.

a steady state solution, even a small viscosity can produce an observable disturbance *preceding* the quark. In the hydrodynamic simulations of [44, 45, 46] the fluid is ideal. Hence, the “shock”-like nature of the quark disturbance is recovered and the energy density is qualitatively different.

In Fig. 3 we superimposed the magnitude and the vector plot of the collective flow \vec{U} . As the quark moves forward, matter is being transported by collective flow in the direction opposite to quark motion. This effect is, in itself, not completely surprising since perturbative calcu-

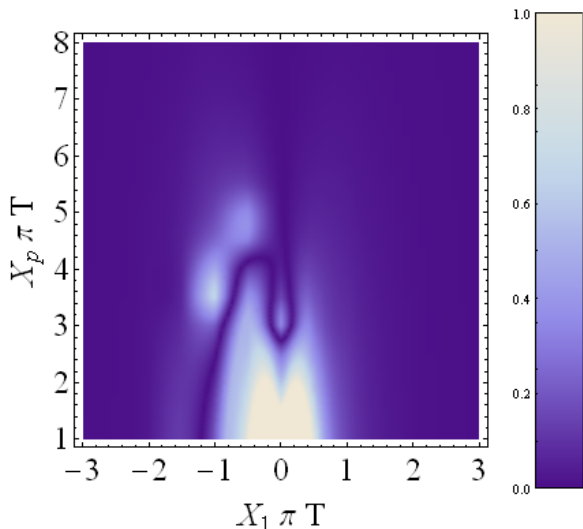


FIG. 4: (Color online) Comparison between the full numerical solution for \vec{U} and the leading order expression in Eq. (12), i.e., $|\vec{U} - \vec{S}/4P_0|$ for $v = 0.99$.

lations [47] admit both momentum flow out of the quark (if repulsive channels dominate) and into the quark (if attractive channels dominate). Furthermore, in a system with no conserved charges, collective flow and heat diffusion can compensate each other since the effect of both is moving energy-momentum throughout the system. This picture, is however very far from the point-like energy source considered in the “text-book” Mach cone example of [20].

In Fig. 4 we compare the full numerical solution of Eq. (8) and the leading order result in Eq. (12). This plot indicates that the system’s dynamics becomes linear outside the narrow region between $-1/\pi T < X_1 < 1/\pi T$ and $0 < X_p < 6/\pi T$. This is in agreement with the result in Fig. 2 because the magnitude of \vec{V} (or \vec{U}) becomes very small outside this region.

Finally, Fig. 5 shows the discrepancy between the Navier-Stokes tensor and $T_{\mu\nu}^Y$ in the Landau frame, which are parametrized by the tensor $Z_{\mu\nu}$ (Eq. 18). As can be seen, the magnitude and structure of the discrepancy remains somewhat the same across all components of $Z_{\mu\nu}$. Outside the region where $-3/\pi T < X_1 < 3/\pi T$ and $0 < X_p < 10/\pi T$ (the quark is at $X_1 = X_p = 0$), the system can be described by the first-order Navier-Stokes energy-momentum tensor to an accuracy of roughly 90%. Inside that region, however, the discrepancy quickly rises and diverges. Note that in the region where Navier-Stokes provides a good description of the system the numerically calculated velocity flow \vec{U} matches the leading order in Eq. (12). This implies that, in this region, the system is better described by the linearized version of the first-order Navier-Stokes equations.

The detailed structure of the divergence is numerically difficult to examine but its sudden onset suggests the

presence of coherent Yang-Mills fields, where deviation from hydrodynamics is at its maximum. Coherent fields do not of course have a comoving frame, but they can be transformed into a frame (which will in general be different than the frame set by U^μ as calculated here) where the energy-momentum tensor given by

$$(T_{\mu\nu}^{coherent}) = \text{diag}\{\rho', p', 0, 0\} \quad (21)$$

(where ρ' and p' are taken to mean energy and momentum flow density, not “true” thermal densities and pressures). Here, the X_1 direction is taken to be parallel to the Poynting vector. The Z_{ii} calculated for this field can go to zero, which results in divergences in ratios of Z ’s as seen in Fig. 5. This indicates that coherent Yang-Mills fields are present in the vicinity of the quark. In fact, note that Yarom’s $\Delta T_{\mu\nu}$ (6) does seem to have a Lorentz contracted Weizsäcker-William-like form but its $\mathcal{O}(T^2/X^2)$ parametric dependence is quite distinct from the vacuum Coulomb behavior [42].

Our results for the components of Z do not significantly change if we increase the intensity of the coupling to $\lambda = 6\pi$. However, at lower quark velocities the Navier-Stokes equations provide an accurate description of the system’s dynamics at distances $\geq 1.5/\pi T$ (see Fig. 6). These results coincide remarkably well with the limit estimated through the uncertainty principle [9].

Fig. 7 confirms that $\Pi_{\mu\nu}$ stays smooth and finite throughout, and the divergence is due to a maximal breakdown of isotropy (one of the Z_{ii} going to zero). Furthermore, Fig. 7 shows that in the regime in which hydrodynamics works, $\Pi_{\mu\nu}$ is a perturbatively small correction to the energy-momentum tensor. The regime where $\Pi_{\mu\nu}$ becomes significant approximately coincides with the regime in which the Navier-Stokes description stops to be a good description of the physical system. Thus, it is unlikely that higher gradient corrections to Navier-Stokes equations (such as [48, 49, 50]) will make a significant difference in our results.

The contours of our figures look non-trivial and no easy interpretation of them can be given here, especially as they are highly susceptible to $1/N_c$ corrections (as remarked in the previous section). The fine detailed structure in the figures is sensitive to the interpolation numerics and only the global features are numerically stable. We remark, however, that the size of the “inner region” is very similar in all the figures and also agrees well with the estimate for the “Knudsen boundary” in Fig. 1. It is therefore worth underlining how the results agree with the expectations described in the previous sections. The system is neatly defined by a Knudsen region where $-3/\pi T < X_1 < 3/\pi T$. Inside this layer, non-equilibrium deviations from the hydrodynamic description dominate. On the other hand, outside this region nearly ideal and linearized hydrodynamics provides an acceptable description of the system.

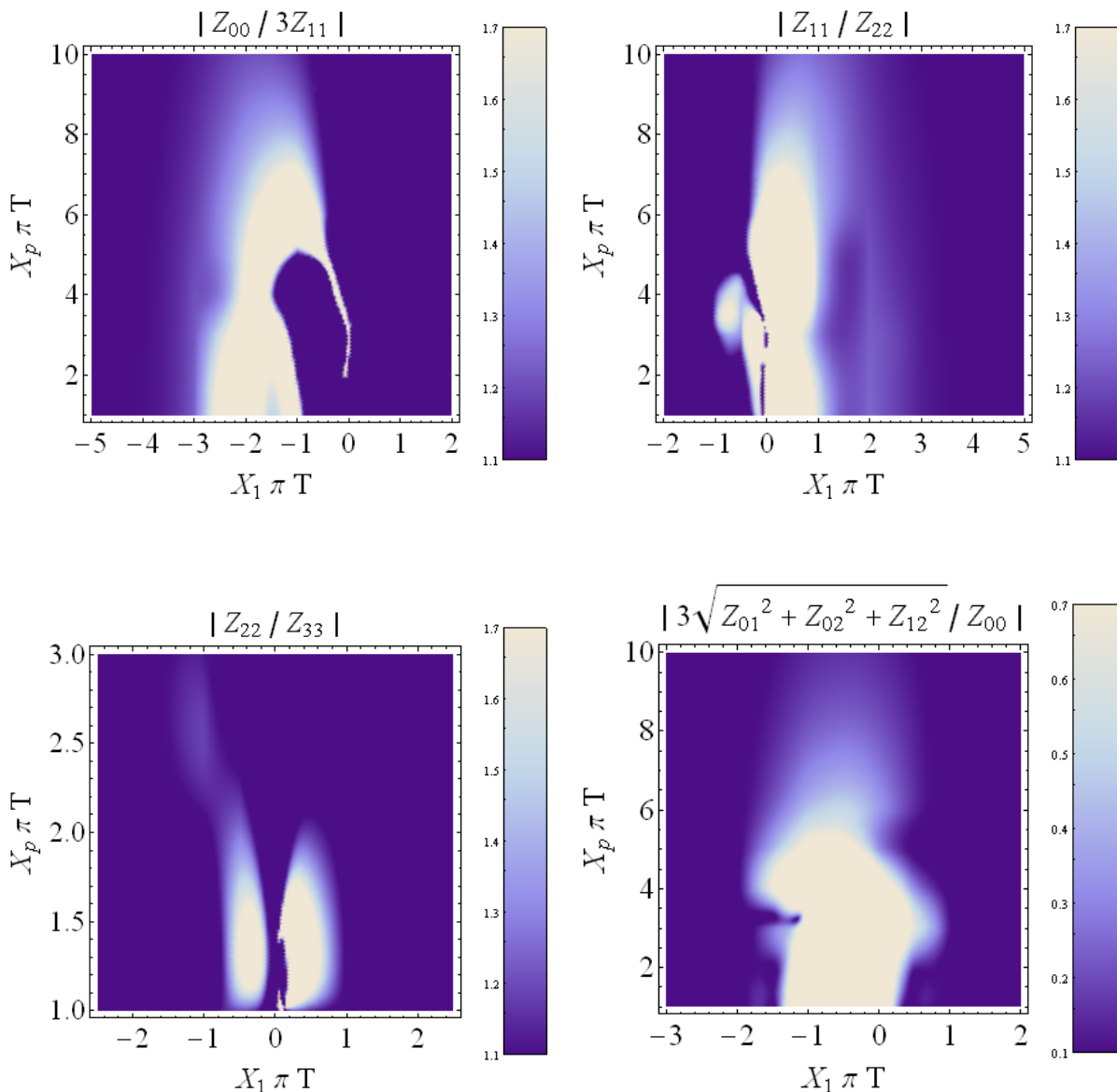


FIG. 5: (Color online) Tests of local equilibrium for the elements of the energy-momentum tensor in the Landau frame. $Z_{\mu\nu}$ is defined in Eq. 18 and $v = 0.99$. Ratio values outside of the limits were color-coded as the limits.

V. CONCLUSIONS

Encouragingly, the scale at which the energy deposited by the jet thermalizes is comparable to the thermalization time constraints obtainable from anisotropic flow measurements [11], which suggests that in the strongly coupled regime the nearly inviscid microscopic dynamics responsible for creating large v_2 such as those seen at RHIC also has the potential to transform the energy of quenched hard jets into flow of soft particles. The short timescale seen in the present work indicates that, provided strongly coupled AdS/CFT is indeed qualitatively similar to sQGP, the energy deposited by jets in the system becomes to a very good approximation locally thermalized.

Second-order hydrodynamic corrections [48] may somewhat change the results presented here. However, as argued previously, the contribution of the relaxation time to collective dynamics might be not so large. Analyses of other systems within the AdS/CFT framework, such as [51], confirm this. An analysis of the presently investigated solution within the second order framework, analogously to that presented in [51, 52] for a Boost-invariant fluid, is currently in progress.

It should be noted that there is to date no universally agreed framework for relativistic hydrodynamics beyond leading order, with several higher order frameworks possible (see, for example, [48, 49, 50] and references within these works). This still unresolved ambiguity might hold the key to explaining some puzzles encountered in trying

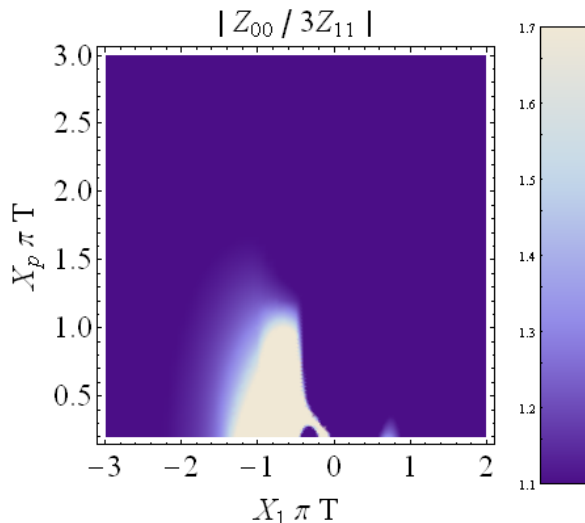


FIG. 6: (Color online) Test of local equilibrium for the elements of the energy-momentum tensor in the Landau frame for $v = 0.75$ and $\lambda = 3\pi$. Z_{00} is defined in Eq. 18. Ratio values outside of the limits were color-coded as the limits.

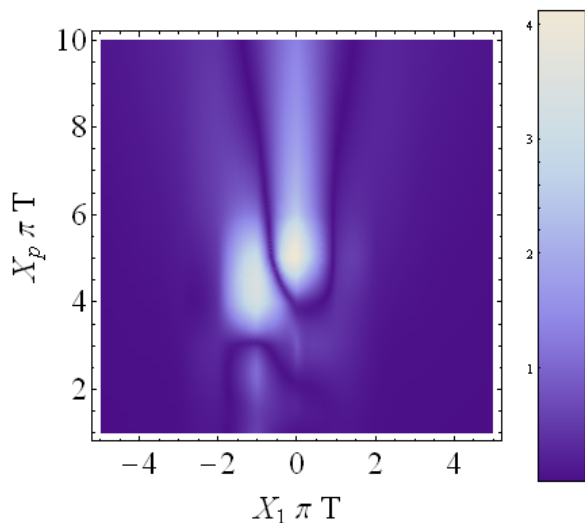


FIG. 7: (Color online) The relative importance of the viscous tensor with respect to the energy-momentum tensor in the Landau frame, $\sqrt{\sum_{\mu\nu} \Pi_{\mu\nu}^2 / \sum_{\mu\nu} Z_{\mu\nu}^2}$, corrected for double-counting. Here $v = 0.99$.

to model heavy ion collisions using non-ideal hydrodynamics (the numerical instabilities encountered in [12], and the very low viscosity encountered in [15]). For a discussion of second-order viscous hydrodynamics in conformal field theories at finite temperature see [53, 54].

We hope that AdS/CFT techniques might help in clarifying the situation by providing a bonafide “analytical”

solution for a strongly coupled relativistic quantum system with none of the approximations, whose validity is questionable at strong coupling, that usually go into the derivation of transport equations. For such a clarification, an analysis of AdS/CFT inspired solutions using methods similar to those described here is necessary. This effort could, independently from AdS/CFT’s applicability to heavy ion collisions, lead to a better comprehension of the general and fundamental problem of the dynamics of strongly-coupled relativistic systems.

In conclusion, in this work we have compared the analytically obtained energy-momentum tensor of a very massive quark moving through a strongly coupled $\mathcal{N} = 4$ SYM plasma with a non-ideal tensor given by the first-order Navier-Stokes ansatz. We have found that the energy deposited by the quark is already thermalized in the region where $|X_1| > 3/\pi T$ and $X_p > 1/\pi T$, which defines a length scale that is considerably shorter than the time-scale of the jet traveling throughout the medium, or the medium’s hydrodynamic evolution. Thus, if strongly coupled $\mathcal{N} = 4$ SYM is an appropriate description of RHIC physics, we have every reason to expect that in the strongly coupled region the missing jet energy has been thermalized. The thermalization timescale is (indeed, the lifetime of the heavy ion system), slightly smaller than the timescale found in [34]. Thus, in view of the results present here, one can say that linearized first-order Navier-Stokes hydrodynamics provides an accurate description of the $\mathcal{N} = 4$ SYM plasma surrounding the heavy quark down to distances of about $3/\pi T$. A quantitative hydrodynamic analysis of the energy deposited in jets at smaller distances needs to be treated nonlinearly, as in [45, 46].

We expect that further progress in examining strongly coupled $\mathcal{N} = 4$ SYM systems will better clarify the thermalization timescale and dynamics of strongly coupled field theories.

VI. ACKNOWLEDGEMENTS

The authors thank A. Yarom for useful correspondence and D. Rischke for useful suggestions. Comments from S. Gubser, J. Casadelrrey-Solana, and P. M. Chesler on the earlier version of this paper are gratefully appreciated. J.N. acknowledges support by the Frankfurt International Graduate School for Science (FIGSS) and Gesellschaft für Schwerionenforschung (GSI). G.T. would like to thank J.W.-Goethe Universität and the Alexander Von Humboldt foundation for the support provided for this research. M.G. and J.N. acknowledge partial support from DOE under Grant No. DE-FG02-93ER40764. M.G. also thanks DFG, ITP, FIAS for partial support.

[1] I. Arsene et al. (BRAHMS), Nucl. Phys. **A757**, 1 (2005).

[2] K. Adcox et al. (PHENIX), Nucl. Phys. **A757**, 184

- (2005).
- [3] B. B. Back et al., Nucl. Phys. **A757**, 28 (2005).
 - [4] J. Adams et al. (STAR), Nucl. Phys. **A757**, 102 (2005).
 - [5] X.-N. Wang, M. Gyulassy, and M. Plumer, Phys. Rev. **D51**, 3436 (1995).
 - [6] M. Gyulassy, I. Vitev, X.-N. Wang, and B.-W. Zhang (2003), nucl-th/0302077.
 - [7] R. Baier, Y. L. Dokshitzer, A. H. Mueller, S. Peigne, and D. Schiff, Nucl. Phys. **B483**, 291 (1997).
 - [8] A. Majumder and X.-N. Wang, Phys. Rev. **C73**, 051901(R) (2006).
 - [9] P. Danielewicz and M. Gyulassy, Phys. Rev. D **31** (1985) 53.
 - [10] M. Gyulassy and L. McLerran, Nucl. Phys. A **750**, 30 (2005).
 - [11] U. W. Heinz and P. F. Kolb, Nucl. Phys. A **702**, 269 (2002).
 - [12] H. Song and U. W. Heinz, Phys. Lett. B **658**, 279 (2008).
 - [13] D. Teaney, J. Lauret and E. V. Shuryak, arXiv:nucl-th/0110037.
 - [14] D. Teaney, Phys. Rev. C **68**, 034913 (2003).
 - [15] P. Romatschke and U. Romatschke, Phys. Rev. Lett. **99**, 172301 (2007).
 - [16] J. M. Maldacena, Adv. Theor. Math. Phys. **2**, 231 (1998); E. Witten, Adv. Theor. Math. Phys. **2**, 253 (1998); **2**, 505 (1998); V. Balasubramanian and P. Kraus, Commun. Math. Phys. **208**, 413 (1999).
 - [17] G. Policastro, D. T. Son, and A. O. Starinets, Phys. Rev. Lett. **87**, 081601 (2001).
 - [18] P. K. Kovtun, D. T. Son, and A. O. Starinets, Phys. Rev. Lett. **94**, 111601 (2005).
 - [19] J. Casalderrey-Solana, E. V. Shuryak and D. Teaney, arXiv:hep-ph/0602183.
 - [20] L. D. Landau, E. M. Lifshitz, *Fluid Mechanics* (Pergamon Press, New York, 1987), Vol. 6.
 - [21] H. Stoecker and W. Greiner, Phys. Rept. **137**, 277 (1986).
 - [22] L. M. Satarov, H. Stoecker and I. N. Mishustin, Phys. Lett. B **627**, 64 (2005).
 - [23] J. Casalderrey-Solana and D. Teaney, Phys. Rev. **D74**, 085012 (2006).
 - [24] T. Renk and J. Ruppert, Phys. Rev. C **76**, 014908 (2007).
 - [25] C. A. Pruneau [STAR Collaboration], J. Phys. G **34**, S667 (2007).
 - [26] J. G. Ulery [STAR Collaboration], Nucl. Phys. A **774**, 581 (2006).
 - [27] A. Adare *et al.* [PHENIX Collaboration], Phys. Rev. C **77**, 011901 (2008).
 - [28] J. J. Friess, S. S. Gubser, and G. Michalogiorgakis, JHEP **09**, 072 (2006).
 - [29] J. J. Friess, S. S. Gubser, G. Michalogiorgakis and S. S. Pufu, Phys. Rev. D **75**, 106003 (2007).
 - [30] S. S. Gubser, S. S. Pufu and A. Yarom, Phys. Rev. Lett. **100**, 012301 (2008).
 - [31] S. S. Gubser and A. Yarom, Phys. Rev. D **77**, 066007 (2008).
 - [32] S. S. Gubser, S. S. Pufu and A. Yarom, arXiv:0711.1415 [hep-th].
 - [33] P. M. Chesler and L. G. Yaffe, Phys. Rev. Lett. **99**, 152001 (2007).
 - [34] P. M. Chesler and L. G. Yaffe, arXiv:0712.0050 [hep-th].
 - [35] A. Yarom, Phys. Rev. D **75**, 105023 (2007).
 - [36] S. S. Gubser and S. S. Pufu, Nucl. Phys. B **790**, 42 (2008).
 - [37] S. S. Gubser, S. S. Pufu and A. Yarom, JHEP **0709**, 108 (2007).
 - [38] C. P. Herzog, A. Karch, P. Kovtun, C. Kozcaz and L. G. Yaffe, JHEP **0607**, 013 (2006).
 - [39] S. S. Gubser, Phys. Rev. D **74**, 126005 (2006).
 - [40] J. Casalderrey-Solana and D. Teaney, JHEP **0704**, 039 (2007).
 - [41] S. S. Gubser, I. R. Klebanov and A. W. Peet, Phys. Rev. D **54**, 3915 (1996).
 - [42] J. Noronha, M. Gyulassy and G. Torrieri, arXiv:0807.1038 [hep-ph].
 - [43] We thank P. M. Chesler for pointing out this result to us.
 - [44] B. Betz, M. Gyulassy and G. Torrieri, Phys. Rev. C **76**, 044901 (2007).
 - [45] H. Stoecker, B. Betz and P. Rau, PoS C **POD2006**, 029 (2006) [arXiv:nucl-th/0703054].
 - [46] B. Betz, M. Gyulassy, D. H. Rischke, H. Stoecker and G. Torrieri, arXiv:0804.4408 [hep-ph].
 - [47] X-N Wang, private discussion and communication.
 - [48] W. Israel and J. M. Stewart, Annals Phys. **118**, 341 (1979).
 - [49] T. Koide, G. S. Denicol, Ph. Mota and T. Kodama, Phys. Rev. C **75**, 034909 (2007).
 - [50] K. Dusling and D. Teaney, Phys. Rev. C **77**, 034905 (2008).
 - [51] M. P. Heller and R. A. Janik, Phys. Rev. D **76**, 025027 (2007).
 - [52] Y. V. Kovchegov and A. Taliotis, Phys. Rev. C **76**, 014905 (2007).
 - [53] R. Baier, P. Romatschke, D. T. Son, A. O. Starinets and M. A. Stephanov, JHEP **0804**, 100 (2008).
 - [54] S. Bhattacharyya, V. E. Hubeny, S. Minwalla and M. Rangamani, JHEP **0802**, 045 (2008).